Spraying Systems Co.®
Experts in Spray Technology

SPRAY TRANSFER EFFICIENCY ONTO A HIGH-SPEED WEB: BOUNDARY LAYER EFFECTS AND MANIPULATION

B. Drummond, K. M. Bade, and R. J. Schick
Spray Analysis and Research Services, Spraying System Co., USA



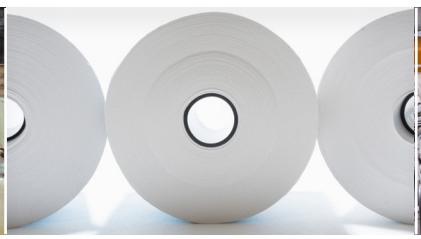


Presented at ICLASS 2018, 14th Triennial International Conference on Liquid Atomization & Spray Systems, Chicago, IL, USA, July 22-26, 2018

Spray Transfer Efficiency onto a High-Speed Web: Boundary Layer Effects and Manipulation

B. Drummond, K. M. Bade*, and R. J. Schick

[1]Spray Analysis and Research Services, Spraying System Co., USA

Abstract

Moving webs are used frequently in the industrial manufacturing world as belts, fabrics, or fiber-based products. In high speed applications, which can be moving upwards of 5000 ft/min, these speeds create a significant boundary layer of moving air. This effect can prevent unwanted buildup on the web surface, but when spraying a liquid solution onto the web surface, such as adding lotion in a tissue making process, this air barrier can present an undesirable challenge. This study characterizes the air barrier, examining: speed, thickness, and shape; and explores techniques to manipulate the boundary for easier application of solution. A test setup with a high-speed belt was constructed, and the boundary later is evaluated using Particle Image Velocimetry (PIV) with and without manipulation. Droplet trajectories and interactions with the belt are investigated. Boundary layer manipulation techniques are applied, and the resulting downstream air barrier is investigated with and without a spray. Physical measurements of the volume of fluid reaching the belt surface are used to quantify the transfer efficiency and the PIV results are used to explain the changes in transfer efficiency across the various air barrier mitigation methods.

Introduction

In the industrial manufacturing world of moving conveyers and liquid sprays are used in conjunction for many different applications, for example: belt cleaning, surface coating, and cooling. As the web (belt) moves, a drag force is applied on the air just above the web surface and a boundary layer is formed overtop of the web. As the web speed increases, the boundary layer may grow as additional momentum is transferred to the surrounding air. At low speeds, spray droplets may have enough momentum to pass through boundary layer and interact with the web surface. At higher speeds, up to 7200 ft/min (36.6 m/s) [1] can be used for tissue making, this boundary layer air provides sufficient drag to overpower the spray droplet trajectories and redirect them downstream, effectively preventing a significant percentage of the droplets from reaching target web surface. This significantly lowers the transfer efficiency of the sprays and will increase the operating costs of the overall manufacturing process. While little work has been done to rigorously examine air-barrier interaction in the paper-making industry, Zhu *et al.* [2] and Guler *et al.* [3] demonstrated that for agricultural applications, wind speeds even less than 1000 fpm (5 m/s) can have significant effects on drift and droplet transfer efficiency, which is 1-7 times lower than paper industry conveyor speeds. A key indicator of sprays with low transfer efficiency is when surrounding equipment or floors become coated in the spray solution that was intended to have been applied to the web. In industry, when operators witness this, some type of deflector is created to slow the incoming boundary layer air and shelter the sprays in an attempt to increase transfer efficiency. Aside from anecdotal evidence, little rigorous examination has been conducted to compare these air barrier mitigation devices to quantify their effects on the process. For the purposes of this investigation and discussion, the term boundary layer refers to the well-defined momentum driven air stream close to the web surface, while the term air-barrier is given to identify the qualitative transfer efficiency reducing air flow near the web surface.

The following research effort mimics the spraying of an additive onto liner-board which is produced to be the outside sheets of cardboard shipping boxes. These lines run between 1000 ft/min to 4000 ft/min depending on the age of the machine, and due to the very low application rates of the additive, external-mix air-atomizing style nozzles are typically used. Air atomizing nozzles utilize compressed air to break up the liquid droplets to create a desired spray pattern. These nozzles spray the liquid from a round orifice that is typically between 0.010 - 0.040" (0.254 - 1.016 mm) in diameter [4]. Directly after exiting the nozzle, the liquid stream is sheared by an air stream that surrounds the liquid jet with a concentric annulus, then two air streams impinge the atomized spray at an angle to create an oval spray pattern shape. Typical pressures for both the liquid and compressed air in these nozzles are between 8-20 psi (0.55-1.38 bar), lower pressures are desirable to prevent fine (small) droplets which are more easily swept away from the conveyor by the air barrier flow.

In the industry, a variety of boundary layer/air barrier mitigation devices have been used on board production machines. A common and simple method is to place a metal plate a few inches upstream of the nozzles spraying

*Corresponding author: Kyle.Bade@spray.com

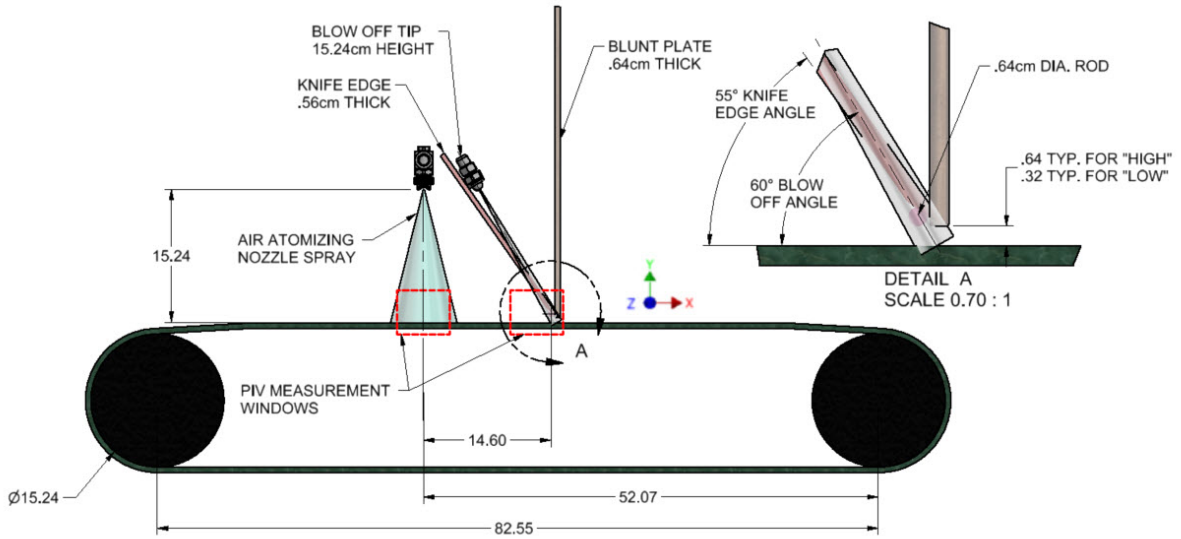

Figure 1: Setup summary of the conveyor, nozzle, spray, and manipulation hardware.

the additive fluid. These mechanical blocking plates are thin and set up in a range of conditions depending on the equipment constraints of the machine. They are placed as close as possible to the moving web without touching it. Another common mitigation method is to use compressed-air blow-off nozzles to create a counter-flow air sheet upstream of the additive spray to disrupt the developed boundary laser from presenting a significant air-barrier. These blow-off nozzles are typically mounted to the same structure as the additive nozzle, so are only a few inches upstream, and are tilted between 20-60 deg upstream off vertical. In addition to these common air-barrier mitigation techniques, a knife-edge plate angled upstream and small diameter rod placed close to the web were tested for comparison; but these are not currently typical methods used in the industry.

Experimental Methods

The high-speed conveyer consists of two larger rollers, 6.0" (15.2 cm) in diameter, and a bed of 25 smaller rollers creating a supported flat section constituting the test-section. The 4" (10.1 cm) wide conveyer loops around the larger drums and is driven by the downstream large roller which is attached to a motor. The conveyer speed was set at 2080 ft/min (10.56 m/s) for all tests performed. The positioning of the spray nozzle and conveyer are show in Figure 1 and the nozzle was oriented to spray vertically down. As the conveyer reaches testing speed an air layer from the moving surface interacts with the spray out of the nozzle, hindering the droplets from reaching the conveyer. Each mitigation device was placed separately with its interaction point of the air layer approximately 110 mm upstream of the centerline of the nozzle to evaluate its effect on the air barrier and resulting transfer efficiency.

The experiment setup focused around a Spraying System Co.® 1/4J+SUE15A external-mix air-atomizing nozzle which features a 0.020" (0.508 mm) diameter fluid orifice. The nozzle was operated at 10 psi (0.7 bar) for both compressed air and liquid for all investigations. As the work focuses on comparing the different mitigation techniques, water at ambient temperature was used as the additive for each test. This nozzle setup pro-duces a volume flow rate of Q_w = 2.2 gal/hr (8.3 lph), and compressed air flow rate of Q_a = 1.65 scfm (45.3 slpm) and is shown in Figure 2.

The boundary layer manipulation methods are shown in Figure 1; which included 1) a baseline case with no manipulation, 2) a blunt plate, 3) an upstream facing knife edge plate, 4) a small cylindrical rod, and 5) a blow-off air-nozzle. The baseline case allows evaluation of the boundary layer without manipulation and assessment of what might constitute an air-barrier. The blunt plate and blow-off nozzle were selected because they are of-ten used in the field, without detailed evaluation of their effect. Finally, the knife-edge and cylindrical rod set-ups were selected to evaluation removal of the boundary layer flow, as well as increased turbulence, respectively.

Two test methods were used to evaluate the boundary layer and transfer efficiency of each mitigation device. The first was Particle Image Velocimetry (PIV) which provides a planar vector field, oriented in the xz-plane. The second was physical collection of the spray from the conveyer surface to measure and compare exactly how much

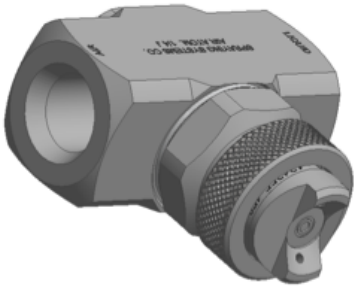

Figure 2: 1/4J+SUE15A air-atomizing external-mix spray nozzle.

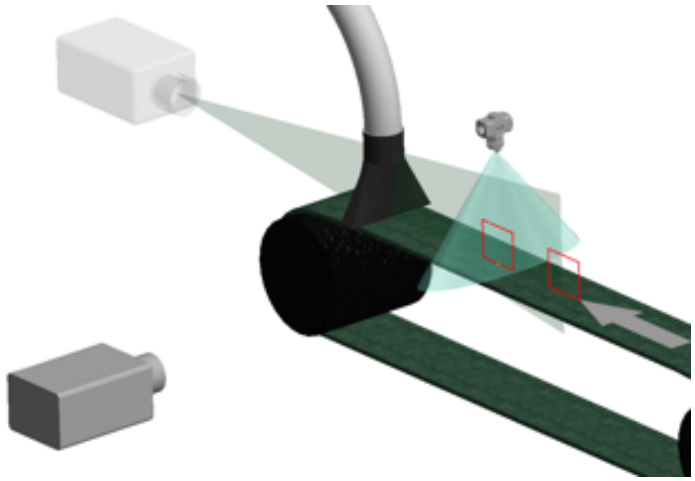

Figure 3: PIV setup with camera, laser, PIV image regions (red). The vacuum setup is also shown, but was not installed during PIV testsing.

fluid is effectively transferred from the nozzle to the conveyer under each set of conditions.

Particle Image Velocimetry (PIV) Setup

Particle Image Velocimetry (PIV) was used to acquire 2D vector fields within the boundary layer allowing investigation of the air flow with and without boundary layer manipulation. These results provide insight into the air flow that later influences the spray trajectories and transfer efficiency. Two image regions were acquired, focusing on the *i*) manipulation region and *ii*) the spray region; the PIV regions are identified in Figures 1 and 3 (the exactly size and location of the PIV planes can be identified in Figure 6).

Figure 3 demonstrates the PIV setup overtop of the conveyor which included a diffused laser sheet and a synchronized camera oriented normal to the PIV laser plane. The PIV system consisted of a Solo PIV Nd:YAG double-pulse laser, a high-speed LaVision Imager Intense camera, and LaVision DaVis 8.0 image acquisition and processing software. The laser sheet is emitted with a nominally Gaussian intensity profile, of which the middle 20% was used, which illuminated the spray in the xz-plane. The laser sheet was approximately 5 mm thick in the measurement regions and will be considered sufficiently thin to represent a two-dimensional spray cross-section for this study. The camera provided double-framed images of 1376x1040 pixels, with a known time delay between images. Image calibration was conducted by acquiring an image of a calibration-sheet with markings of known size and spacing to correct the pixel-based images to real-world dimensions. Cross-correlation between the image-pairs allows determination of displace, and associated velocity, of the <10um tracer particles. The oil-based particles were introduced from one corner of the room until a sufficient nominally uniform seed concentration was dispersed in the testing room.

A sample of 200 double-frame images were acquired with time delays of 15, 50, and 125 μs for each setup in each region; each batch of 200 instantaneous vector field was averaged to provide a single ensemble average flow field. The acquisition of PIV data at a range of time delays allowed accurate PIV processing for the wide range of velocities, from over 10 m/s near the conveyor surface, to approximately 0.1 m/s far from the surface.

The PIV vector field calculations used cross-correlations with multi-pass constant-size windows of 32x32 pixels, 1:1 weight, 75% overlaps, and 2 passes. These steps provided a vector resolution of 0.36 mm/vector and 0.37 mm/vector in the upstream and downstream planes, respectively. Vector field post-processing utilized a median filter to remove and replace vectors with an average >2 standard deviations of its neighbors, and remove groups with <5 vectors.

Transfer Efficiency (Fluid Collection) Method

In order to extract transfer efficiency results, fluid collection testing was conducted with the goal to collect only the water that was deposited on the conveyer surface by the fluid nozzle. The collection was achieved using a compressed air vacuum tube at 85 psi and outfitted with a commercial shop-vac (Rigid WD1851) wet surface attachment that was positioned just above the conveyer surface and spanned the width of the conveyor. The position of the vacuum in relation to the fluid nozzle is shown in Figure 3. The vacuum tube was connected directly to the wet surface attachment and had 3 ft of 1" diameter rigid tubing directing the water and air into a

collection chamber which contains a fine-fibre filter to separate the water from the air during the timed collection period. This collection chamber was weighed before and after each test to determine the amount of water collected, and the associated volume flow rate. All water collecting on the upstream face of the vacuum was collected and removed to prevent any dripping onto the conveyer and artificially increasing the collected volume. This collection test was performed for a baseline of no mitigation device for 1 minute and repeated 4 times. Then each mitigation device was placed in position and the collection test was repeated. Finally, due to the spray pattern of the fluid nozzle being wider than the conveyers surface, some amount of water was over-sprayed and needed be excluded from the volume transfer calculation. During the baseline test, the collection chamber and filter were used to directly capture the spray out of the nozzle that fell adjacent to the conveyer for 1 minute. This test was repeated and conducted on both sides of the conveyer.

Results and Discussion

The results of both PIV measurement regions are joined into a single figure for each setup to facilitate assessment of the flow character near the boundary layer manipulation device (PIV region 1) as well as the interaction region between the spray and the conveyor (PIV region 2). In Figures 6-14 the PIV results are presented for many of the examined cases, in each figure, the presented results elements are:

- PIV vectors in blue with the size relative to the flow velocity magnitude. The number of vectors is down-sampled by 4 for easier viewing.
- The gray-scale background is representative of the velocity magnitude.
- The light-gray lines are streamlines calculated with the u and v vectors.
- The red lines are the boundary layer streamwise velocities at each 10 mm streamwise increment.
- The thick black line is the edge of the boundary layer, i.e. the boundary layer thickness (δ)

The results of Figures 6-10 demonstrate the boundary layer characteristics without a spray, and Figures 11-14 provide the spray velocity characteristics in the downstream PIV region (-187<x<-128). Note, the with-spray results were acquired with no general air seeding, while the no-spray results utilized seeding through the testing room.

The boundary layer thickness,

$$\delta(x) = y\left(\frac{u(y)}{U_C} = 0.05\right), \tag{1}$$

where U_C represented the conveyor velocity of 10.56 m/s, represents the wall-normal location where the streamwise velocity reaches 5% of the conveyor speed; at a given x location. The boundary layer thickness provides a direct indicator of the effect of each boundary layer manipulation method. In Figure 4, the boundary layer thickness is provided across both PIV measurement regions for the baseline and all manipulation arrangements. The baseline (black) result demonstrates that the boundary layer thickness is fairly constant across both measurement region and is approximately 22.5 mm. The blow-off nozzle (blue) demonstrates a significant increase in the boundary layer

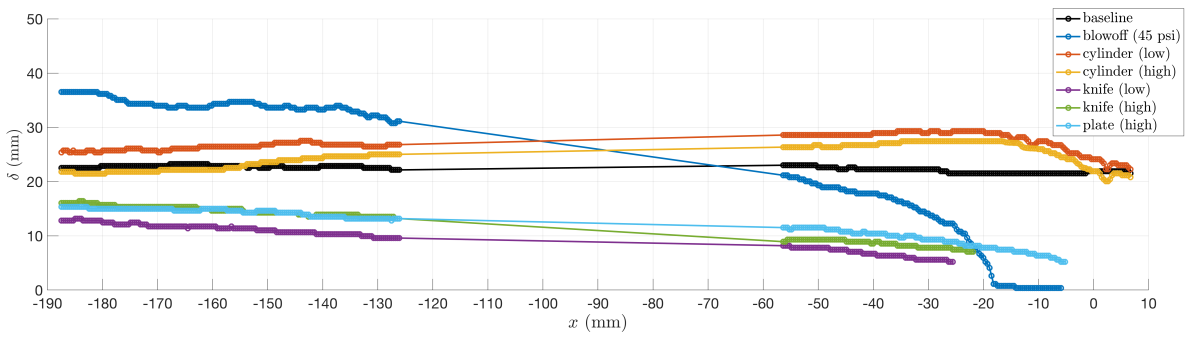

Figure 4: Thickness of the boundary layer for each manipulation setup.

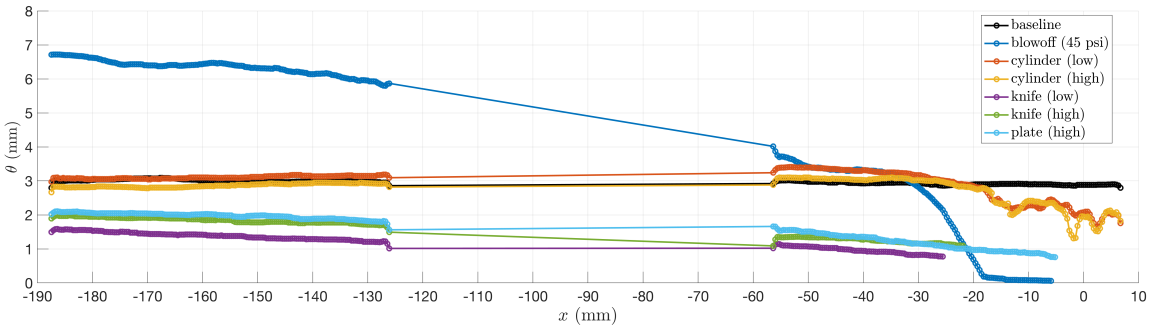

Figure 5: Momentum thickness ($\theta(x)$) of the boundary layer for each manipulation setup.

thickness with an increase of 62%. The cylinder was examined with 3.175 and 6.35 mm gap below the cylinder (low-red and high-orange, respectively), and both cases show an initial boundary layer growth as the flow bends around the top-side of the cylinder, with the boundary layer slowly recovering in the spray region to a similar thickness as the baseline case. Finally, the blunt plate (cyan) and knife-edge with 3.175 and 6.35 mm gap sizes (low-purple and high-green) each demonstrate a reduced boundary layer thickness in the downstream region to 15.8, 12.8 and 16.0 mm, or 30%, 43%, and 29% reductions, respectively.

In order to process the results into a more robust, and perhaps more instructive metric, the momentum thickness,

$$\theta(x) = \int_0^\infty \frac{u(y)}{U_C}\left(1 - \frac{u(y)}{U_C}\right) dy, \tag{2}$$

is calculated and presented in Figure 5 for all test cases. Momentum thickness is preferable metric for determining the potential influence of the boundary layer flow on the spray trajectory for two reasons. First, it is an integral quantity calculated across the boundary alter and is therefore more robust than the direct boundary layer thickness. Second, and more importantly, the momentum thickness provides an assessment on the effective momentum state of the boundary layer, and with this investigation's focus on the ability of the boundary layer to redirect the spray droplets, momentum (i.e. drag) is an attractive and possibly more representative metric. As can be seen in Figure 5, the arrangement from high to low momentum thickness in the spray region actually follows what was observed for the boundary layer thickness. However, the results are smoother and amplified in their difference from the baseline (black) case, where θ=3.0; with the blow-off case increasing by 123% from the baseline and the knife-edge at the low-position decreasing by 53% from the baseline.

The results from the fluid collection testing are provided in Table 1. These results agree with the investigated trends from the PIV analysis very well. The knife-edge results increased the transfer efficiency the most by 42-45% depending on the gap distance. The knife-edge setup provides an interesting arrangement by moving the boundary layer air away from the wall, forcing a back-fill behind the plate resulting in reversed flow and a further decrease in boundary layer velocity. The blunt plate also performed well, increasing the transfer efficiency by 32% over the baseline case. The larger improvement of the knife-edge setup relative to the blunt plate setup is likely due to the upstream-facing knife-edge plate having its downstream-edge closer to the spray nozzle, resulting in a more complete blockage of airflow around the spray, whereas the blunt plate setup leaves a larger gap for entrained air to backfill and begin disrupting the spray further away from the plate. This analysis is un-confirmed since this region was too far from the plate to be captured in the PIV data field of view.

The rod setup had a notable influence near the rod but did not have a persistent effect downstream at the location of the spray. This is reflected in the $\pm$3% change from baseline, a negligible amount. Finally, the blow-off setups had the worst effect in spray transfer efficiency actually reducing the transfer efficiency by 16 and 26%, where the higher air pressure (and flow) caused the largest reducing in volume transfer. As was observed in the boundary layer thickness and momentum thickness results, causing the blow-off nozzle setup to *i*) increase the boundary layer thickness allowing the air-barrier to interact with the spray for a longer time and over a larger space, increasing the altered spray trajectory away from the web surface. And *ii*) the blow-off nozzle actually added high-momentum air flow to the boundary layer, causing an increase in high-momentum fluid as can be seen in Figure 8. This increase moved the bulk spray trajectory downstream, as can be seen in the spray-region of the

Setup	Transfer Efficiency	Change from baseline(%)
Knife -Edge (0.25" gap)	45%	45%
Knife -Edge (0.125" gap)	44%	42%
Blunt-Plate (0.25" gap)	41%	32%
Rod (0.25" gap)	32%	3%
Baseline	31%	N/A
Rod (0.125" gap)	30%	-3%
Blowoff (25 psi)	26%	-16%
Blowoff (45 psi)	23%	-26%

Table 1: Volume collection and transfer efficiency results.

PIV results when comparing the baseline data (Figure 11) to the blow-off data (Figure 13). Also, it appears from the most downstream portion of Figure 13, that the high-velocity spray leaves the PIV region at a higher position, which would likely lead to an increased in lost spray fluid.

Summary and Conclusions

An investigation into the transfer efficiency of spray fluid was carried out to examine the effects of potential boundary layer manipulation hardware. Detailed PIV data were acquired in the boundary layer manipulation region as well as the spray/conveyor interaction region. Evaluation of the boundary layer thickness and momentum thickness provided insight into which mitigation techniques increase or decrease the size and strength of the air-barrier near the high-speed web surface. It was found that the most influential air barrier mitigation techniques were the knife-edge plate which produced a boundary layer momentum thickness decrease of 53%, and the blow-off nozzle which increased the momentum thickness by 123%. Physical collection of the spray material from the surface of the high-speed web allowed for evaluation of the actual transfer efficiency produced by each arrangement. The knife-edge technique was the most successful, producing an increase in transfer efficiency of up to 45% relative to the baseline. It was also shown that the blow-off nozzle reduced the transfer efficiency by up to 26%. Interestingly, the blow-off nozzle is one of two techniques in use in the industry. It is possible that a blow-off nozzle directed downward through the spray could help to increase the transfer efficiency, but this study clearly shows that this method can do more harm than good. The other technique often used is a vertical blunt plate, which was shown to increase transfer efficiency by up to 32% here, and the recommendation for this arrangement is that by tiling the plate upstream, an increase in transfer efficiency is likely to occur.

Acknowledgements

The authors thank Krunal Patel of Spraying Systems Co. for his extensive work on data collection and post-processing in support of this investigation, as well as Bernard Pyzdrowski of Spraying Systems Co. for his efforts in support of this work. Thank you to Kathleen Brown, Wojciech Kalata, and Anthony Perri of Spraying Systems Co. for their past work and consultation which served as a precursor the present investigations.

References

[1] Kullander, J., *Evaluation of Furnishes for Tissue Manufacturing*, Licentiate Thesis, 2012.

[2] Zhu, H., Reichard, D.L., Fox, R.D., Brazee, R.D., and Ozkan, H.E., *Simulation of drift of discrete sizes of water droplets from field sprayers*, American Society of Agricultural and Biological Engineers - Trans. ASAE, 37(5), pp. 1401-1407, 1994.

[3] Guler, H., Zhu, H., Ozkan, H.E., Derksen, R.C., Yu, Y., Krause, C.R., *Spray Characteristics and Drift Reduction Potential with Air Induction and Conventional Flat-Fan Nozzles*, American Society of Agricultural and Biological Engineers, Trans. ASAE, 50(3), pp. 745-754, 2007.

[4] Spraying Systems Co., *Automatic & Air Atomizing Spray Nozzles*, Catalog 76 AA-AUTO, 2015.

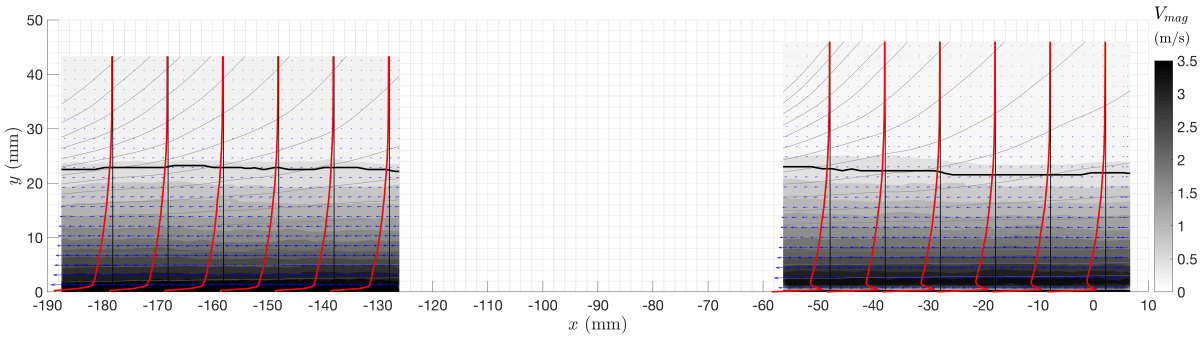

Figure 6: Baseline PIV (no manipulation) results with no spray.

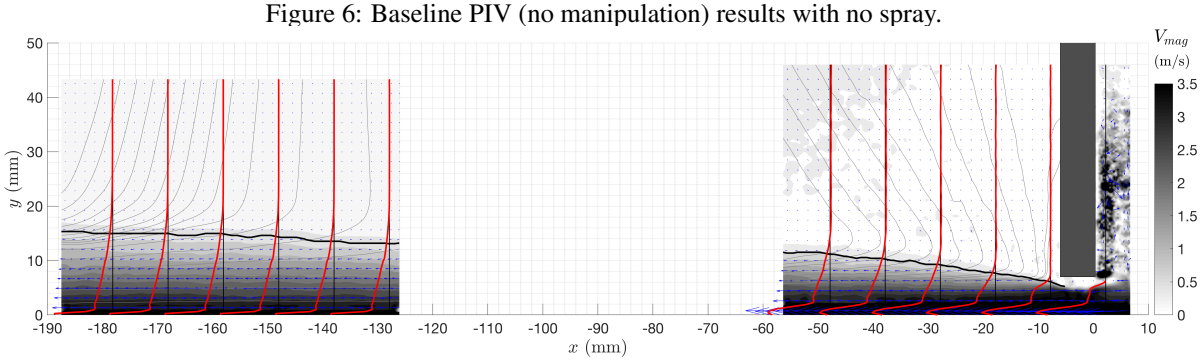

Figure 7: PIV results with the blunt plate located 25mm from the surface with no spray.

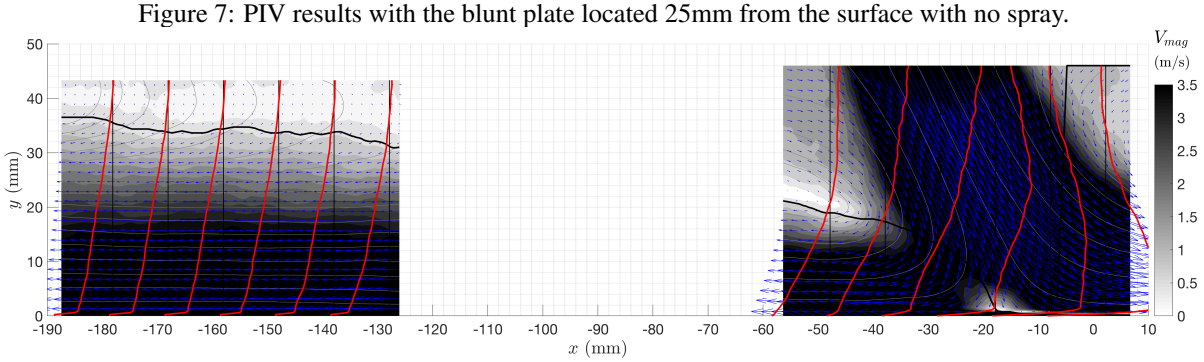

Figure 8: PIV results with the blow-off nozzle at 45 psi with no spray.

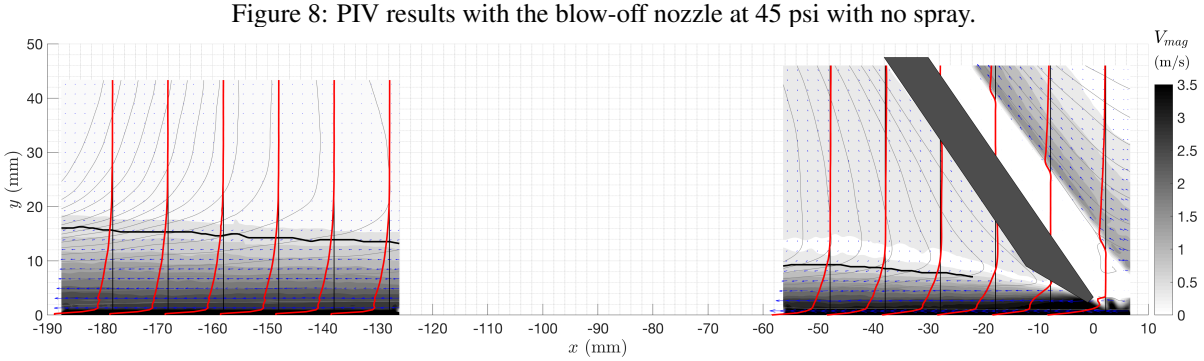

Figure 9: PIV results with the upstream-facing knife-edge located 25mm from the surface with no spray.

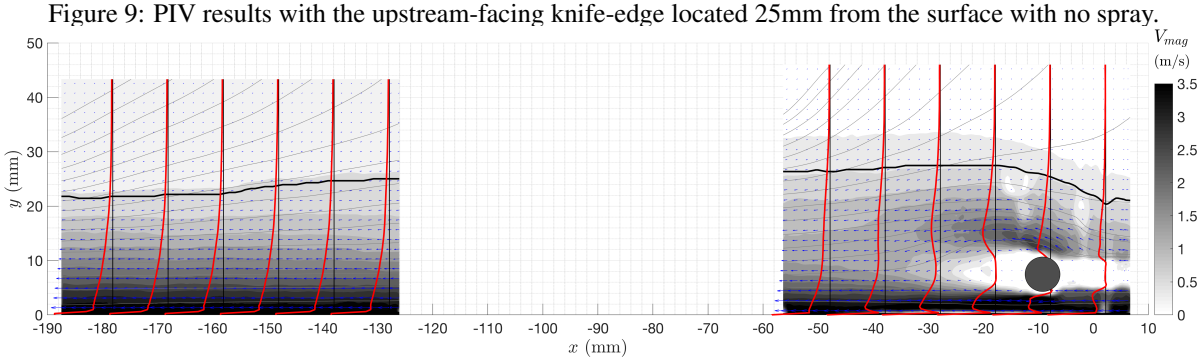

Figure 10: PIV results with the cylindrical rod located 25mm from the surface with no spray.

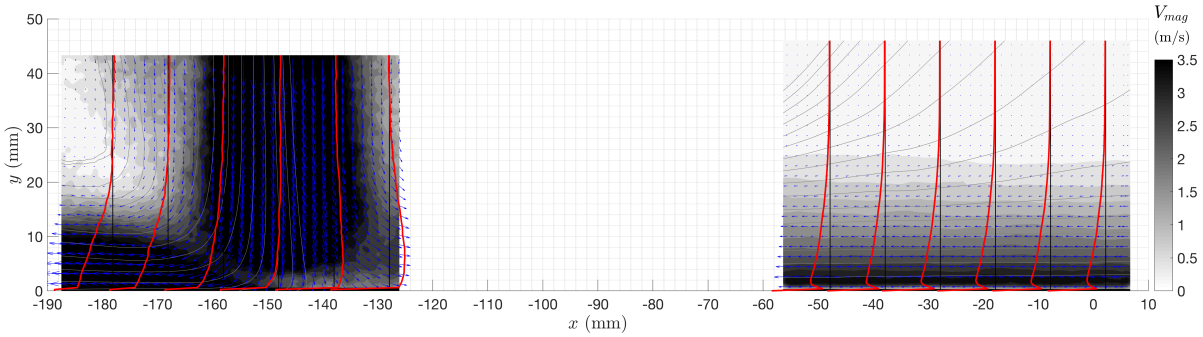

Figure 11: Baseline PIV (no manipulation) results with spray.

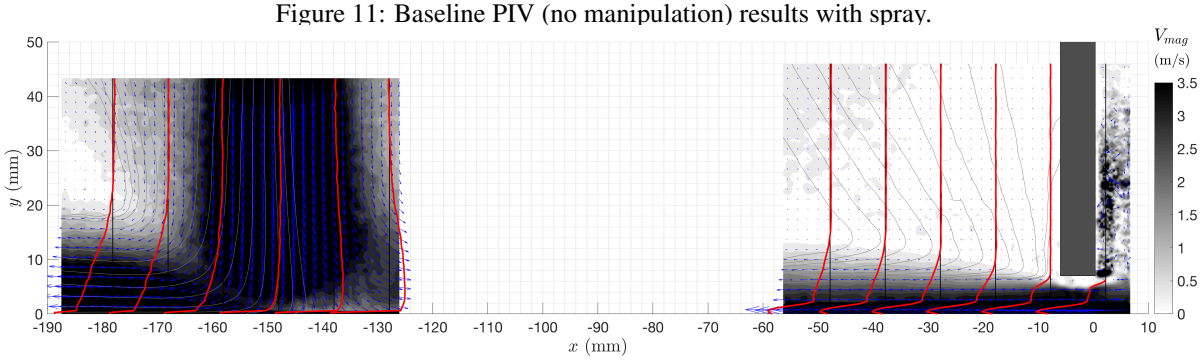

Figure 12: PIV results with the blunt plate located 25mm from the surface with spray.

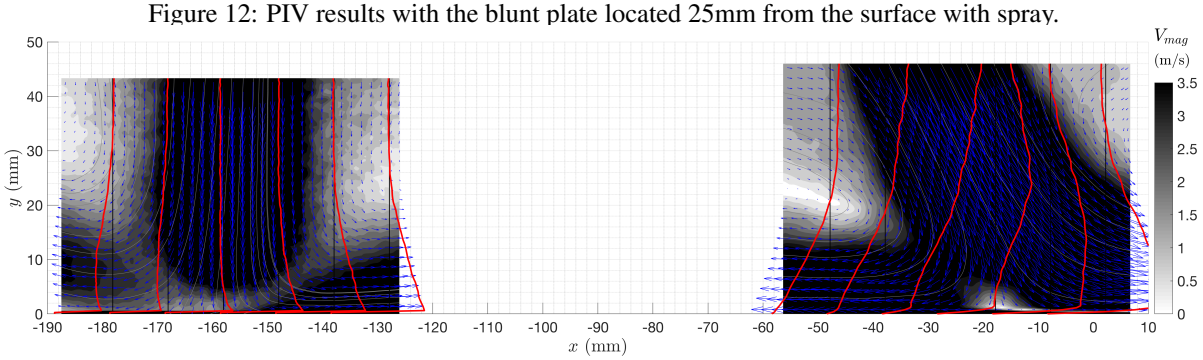

Figure 13: PIV results with the blow-off nozzle at 45 psi with spray.

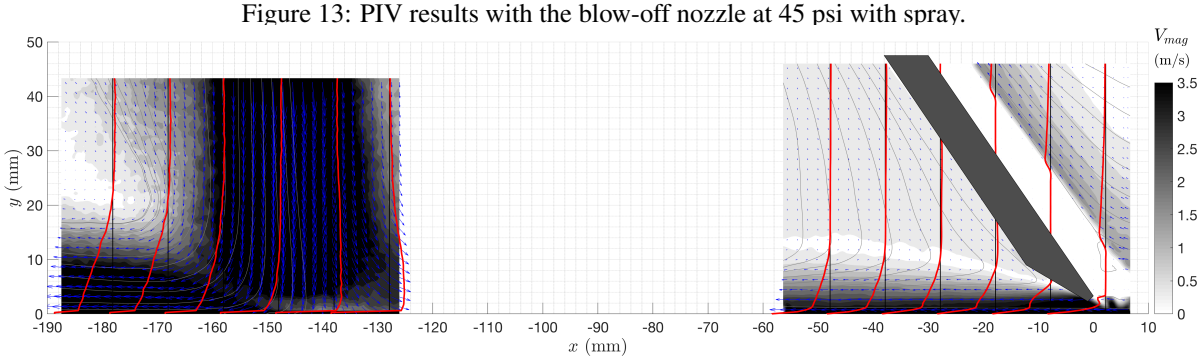

Figure 14: PIV results with the upstream-facing knife-edge located 25mm from the surface with spray.

Spraying Systems Co.®
Experts in Spray Technology

North Avenue and Schmale Road, P.O. Box 7900, Wheaton, IL 60187-7901 USA

Tel: 1.800.95.SPRAY Intl. Tel: 1.630.665.5000
Fax: 1.888.95.SPRAY Intl. Fax: 1.630.260.0842

www.spray.com